

COMITATO NAZIONALE PER L'ENERGIA NUCLEARE  
Laboratori Nazionali di Frascati

LNF - 65/36  
27 Ottobre 1965.

U. Bizzarri, M. Conte, I. F. Quercia and A. Turrin: THE EXTERNAL  
BEAM OF THE FRASCATI ELECTRON SYNCHROTRON. -

(Nota interna: n. 292)

Servizio Documentazione  
dei Laboratori Nazionali di Frascati del CNEN  
Casella Postale 70 - Frascati (Roma)

Nota interna: n. 292  
27 Ottobre 1965.

U. Bizzarri, M. Conte<sup>(x)</sup>, I. F. Quercia and A. Turrin: THE EXTERNAL BEAM OF THE FRASCATI ELECTRON SYNCHROTRON. -

(Presented at the V International Conference on High Energy Accelerators, Frascati, September 1965; Submitted for publication to "Il Nuovo Cimento").

SUMMARY. -

The beam extraction from the Frascati electron synchrotron has been accomplished by exciting the  $\nu_r = 2/3$  non linear betatron resonance.

The second harmonic pattern of the "sextupolar" perturbation in the guiding field which is required to bring the radial oscillations into resonance is introduced by pulsing currents into few wires of the pole face windings of the four quadrants, connected in a loop.

In this way the beam is brought into a two-magnet with septum deflecting channel and escapes completely from the magnetic field.

The extraction channel is described; the preliminary characteristics of the external beam, the results of measurements on the extraction efficiency and the spill-out times obtained are presented.

---

(x) - Now at Rutherford High Energy Laboratory, Chilton, Berks.

## 1. - THEORETICAL INTRODUCTION. -

In order to acquire slow extraction of the beam from cyclic accelerators with high efficiency, low emittance and small momentum spread, the radial betatron oscillations must be brought into resonance<sup>(1-6)</sup>. Long spill-out times, on the other hand, are achieved by means of nonlinear perturbations.

In the following discussion we will limit ourselves only to constant gradient synchrotrons. As it has been shown by one of us (A. T.)<sup>(7)</sup>, the most convenient resonance to get the above mentioned important features is the  $\nu_r = 2/3$  one (consider also references 3-5). The corresponding  $\Delta n(x, \theta)$  perturbation to be introduced must have the following form:

$$(1.1) \quad \Delta n = \left(\frac{dn}{dx}\right) x \sin 2\theta; \quad \left(\frac{dn}{dx}\right) = \text{constant}; \quad \left| \left(\frac{dn}{dx}\right) x \right| \ll \langle n \rangle.$$

If the synchrotron is a circular one, the resulting equation of the radial particle motion

$$(1.2) \quad \frac{d^2 x}{d\theta^2} + (1 - \langle n \rangle) x = \frac{1}{2} \left(\frac{dn}{dx}\right) x^2 \sin 2\theta \quad \left( \begin{array}{l} \langle n \rangle = n_{\text{res}} + \delta \\ n_{\text{res}} = 5/9 \\ |\delta| \ll \left| \left(\frac{dn}{dx}\right) x \right| \end{array} \right)$$

can be integrated by the method of Krylov and Bogoliubov. The first approximation solution is

$$(1.3) \quad x = a(\theta) \sin \left[ \frac{2}{3} \theta + \Phi(\theta) \right] \quad (a(\theta) \geq 0)$$

where  $a$  and  $\Phi$  are related by the following equation<sup>(x)</sup>:

$$(1.4) \quad \cos 3\Phi = \left[ \cos 3\Phi_0 - \frac{3}{2} \left(\frac{\alpha}{a_0}\right) \left[ \frac{(a_0/\alpha)}{(a/\alpha)} \right]^3 + \frac{3}{2} \left(\frac{\alpha}{a}\right) \right]; \quad \alpha = \left| \frac{8\delta}{(dn/dx)} \right|$$

(x) -  $a$  and  $\Phi$  can be found by solving the system

$$(i) \quad \begin{cases} \frac{da}{d\theta} = \frac{3}{32} \left(\frac{dn}{dx}\right) a^2 \sin 3\Phi \\ \frac{d\Phi}{d\theta} = \frac{3}{32} \left(\frac{dn}{dx}\right) a \cos 3\Phi - \frac{3}{4} \delta \end{cases}$$

which furnishes the following simple differential relationship

$$(ii) \quad \frac{d\Phi}{da} = \frac{a \cos 3\Phi - \alpha}{a^2 \sin 3\Phi}; \quad \alpha = \left| \frac{8\delta}{(dn/dx)} \right|$$

Equation (ii) can be expressed by

$$(iii) \quad \frac{dy}{da} + 3 \frac{y}{a} - 3 \frac{\alpha}{a^2} = 0 \quad (y = \cos 3\Phi)$$

and its general integral is just the equation (1.4) of the text.



4.

with  $a_0/\alpha$  and  $\Phi_0$  initial values for the scaled amplitude  $a/\alpha$  and the phase  $\Phi$ .

The last term in equation (1.4) obviously represents the asymptotic behaviour of the solutions when  $a \rightarrow \infty$ .

In fig. 1 a family of curves derived from (1.4) shows  $\cos 3\Phi$  as function of  $a/\alpha$ , corresponding to various initial values of  $a/\alpha$  and  $\cos 3\Phi$ .

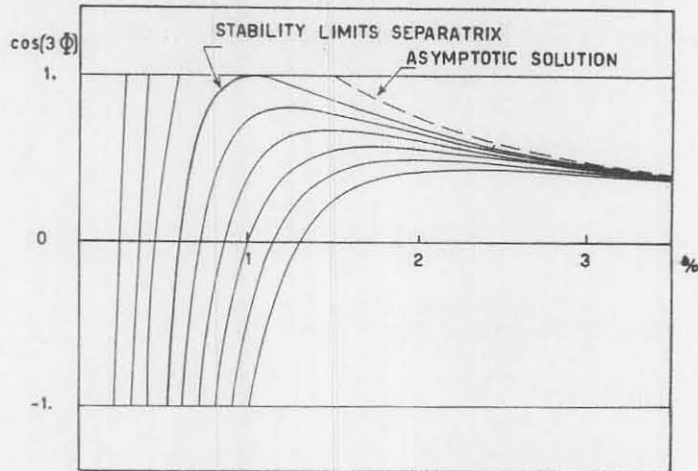


FIG. 1 - Curves corresponding to various initial values  $a_0/\alpha$  and  $\cos 3\Phi_0$  are represented in the  $\cos 3\Phi$  vs.  $a/\alpha$  plot. The separatrix curve (1.5) corresponds to the boundary between limited orbits and resonant orbits regions.

Each curve in fig. 1 is to be imagined travelled by the representative point in a direction which depends from the initial values  $a_0/\alpha$  and  $\Phi_0$ . The curves on the left of the boundary curve

$$(1.5) \quad \cos 3\Phi = -\frac{1}{2}\left(\frac{\alpha}{a}\right)^3 + \frac{3}{2}\left(\frac{\alpha}{a}\right)$$

correspond to permanently limited orbits, whose amplitudes fluctuate between limits given by the intersections with the two lines  $\cos 3\Phi = \pm 1$ .

Curves on the right of the (1.5) curve exhibit the asymptotic behaviour. For an infinite amplitude the asymptotic value of  $\Phi$  is  $\pi/6$  (refer to fig. 2).

Orbit enlargement occurs anyway when  $\frac{a}{\alpha} > 1$  or, in other words,

$$(1.6) \quad \left| a \left( \frac{dn}{dx} \right) \right| > | 8\delta | \quad (\text{refer also to ref. (7)}).$$

Following the above considerations the electron beam has been extracted from the Frascati electron synchrotron in the following way:

At the end of the acceleration cycle, the magnetic perturbation

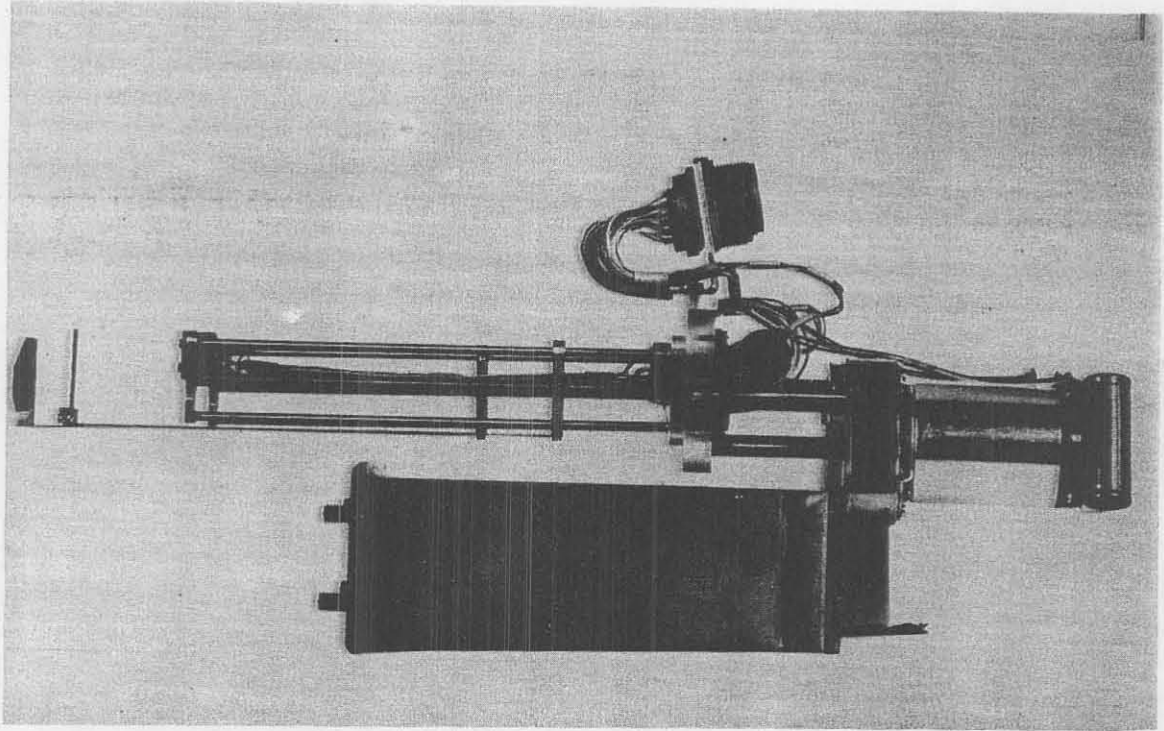


FIG. 4 - Two-targets device for detecting the resonant behaviour of radial oscillations. On the left there is the 5 mm width target, which simulates the mouth of the extraction channel. On the right there is the 1 mm width target, which is nearer to the central orbit and represents the septum thickness. These targets are displaced by 6 cm azimuthally. Their position controlling system is also shown on the right side.

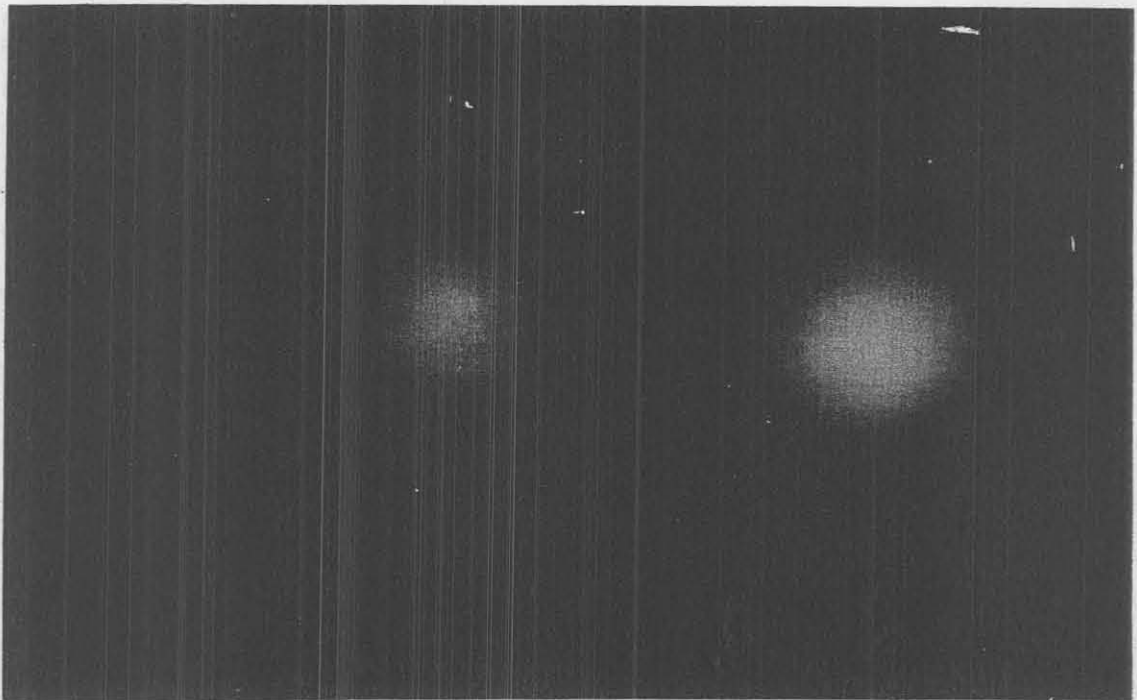


FIG. 5 - Film exposure at about 3 m from the two targets, while the perturbation is applied. The left spot represents the  $\gamma$  ray beam (extracted electrons) coming from the 5 mm target. The right one represents the  $\gamma$  ray beam from the 1 mm target. In this case the extraction efficiency is about 20%.

is introduced, but all the particle oscillations remain limited since their motions are described by the amplitude-limited curves. Growth of oscillations occurs only when the R. F. peak voltage is made to decrease slowly and electrons are allowed to spiralize smoothly inward.

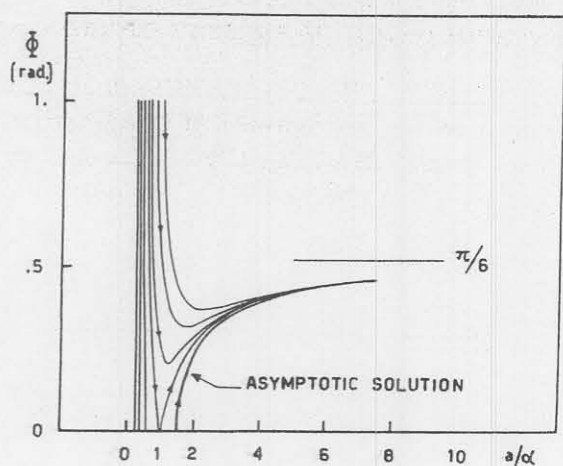


FIG. 2 - Plot of  $\Phi$  vs.  $a/\alpha$ . The asymptotic value of  $\Phi$  is shown to be  $\pi/6$  for an infinite amplitude.

Because of the existing variation in the  $\langle n \rangle$  value along the radial width of the gap,  $\langle n \rangle$  approaches gradually to  $n_{res}$  when the radius of the orbits is made to decrease.

In this way, as soon as condition (1.6) is satisfied, the electron motion becomes controlled by the resonant action of the field, and every particle rushes towards the mouth of the extraction channel in the course of a few revolutions.

## 2. - EXTRACTION OF THE BEAM FROM THE FRASCATI SYNCHROTRON.

The perturbation (1.1) is accomplished by injecting currents at the end of the acceleration cycle into pairs of wires belonging to the pole face windings, connected in an antiinductive loop. Current flows of opposite direction are fed into pairs of wires symmetrically placed with respect to the central orbit, as it is shown in fig. 3. The required azimuthal second harmonic variation of the perturbation is obtained by reversing the direction of the current flows into the wires in each next quadrant of the synchrotron magnet.

If the distances between the wires and the center of the gap are sufficiently large, the desired "sextupolar" perturbation of the field is easily obtained. The shape of the  $\Delta B_z(x)$  obtained in this way is represented in the upper part of fig. 3.

When the perturbing term  $\frac{4}{\pi} \Delta B_z(x) \sin 2\theta$  is introduced, the corresponding equation of motion is:

$$(2.1) \quad \frac{d^2 x}{d\theta^2} + (1 - \langle n \rangle) x = \frac{R}{B_0} \frac{4}{\pi} \Delta B_z(x) \sin 2\theta.$$

The second harmonic variation of  $\Delta B_z(x=0)$  does not cause any resonant effect (it produces only a slight distortion of the closed orbit). It is the parabolic shape of  $\Delta B_z(x)$  that is responsible of the resonance.

A simple device has been used to test whether the particles, under the action of the above described perturbation, are able to jump over a few millimeter radial obstacle.

6.

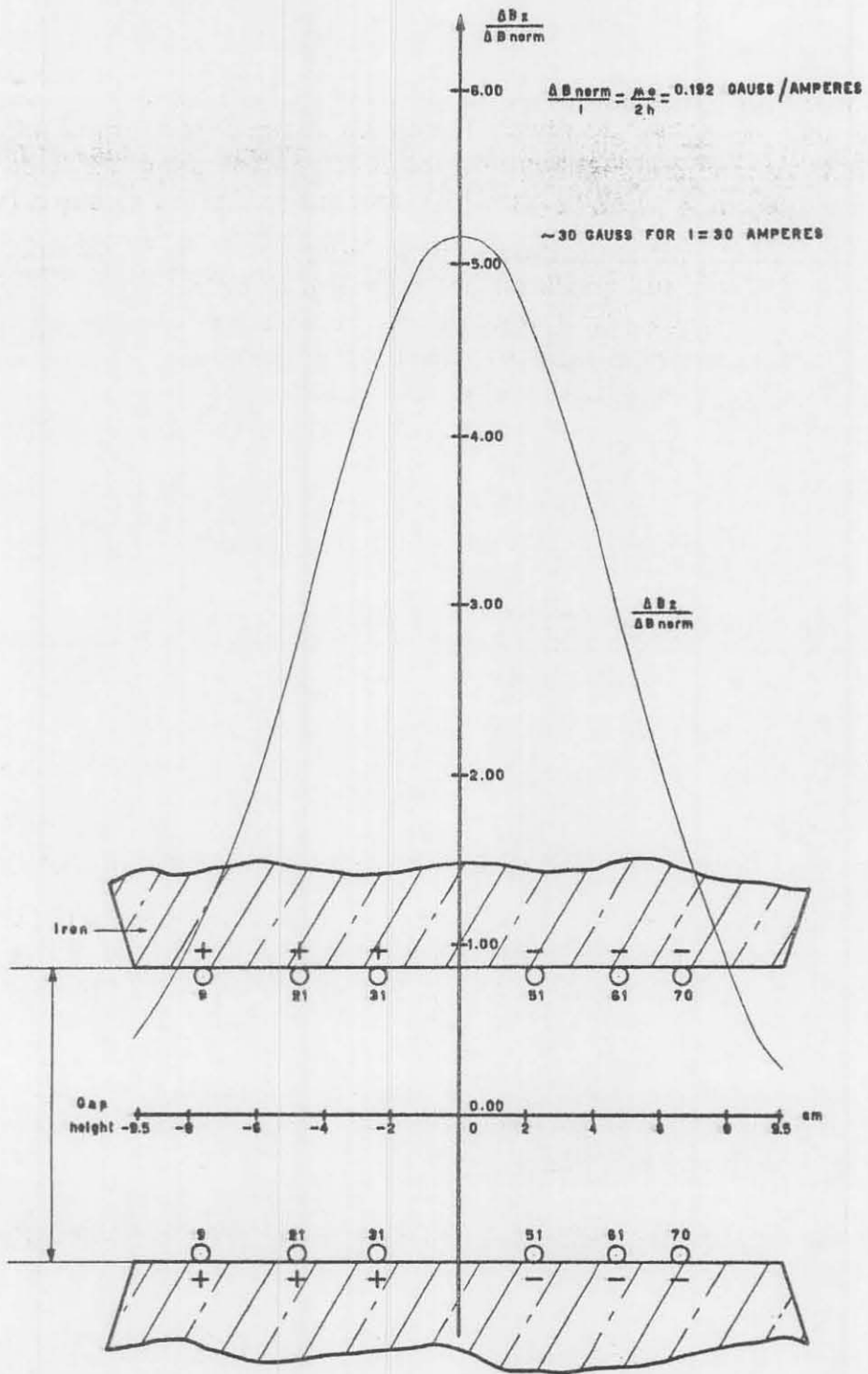


FIG. 3 - Cross section of the Frascati synchrotron's gap. The chosen pairs of wires of the pole face windings are represented. The corresponding  $B_z(x)$ , shown in the upper part of the figure, is measured in arbitrary units.



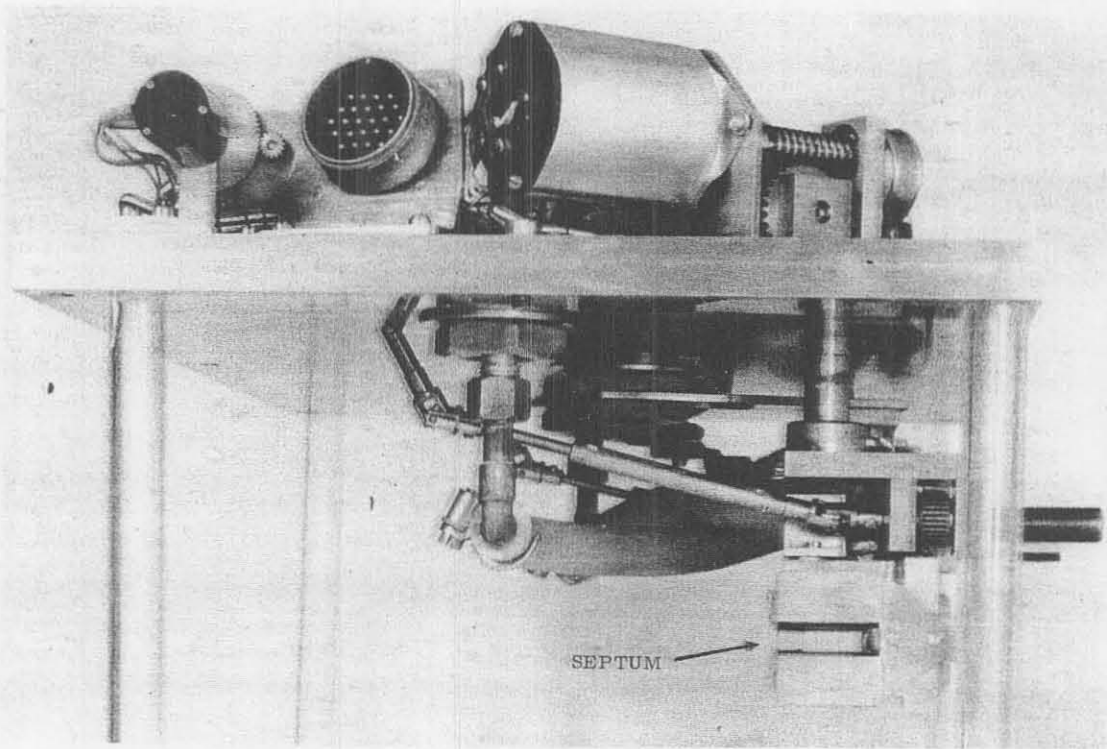


FIG. 8 - "Soft" magnet and its position controlling system (front view).

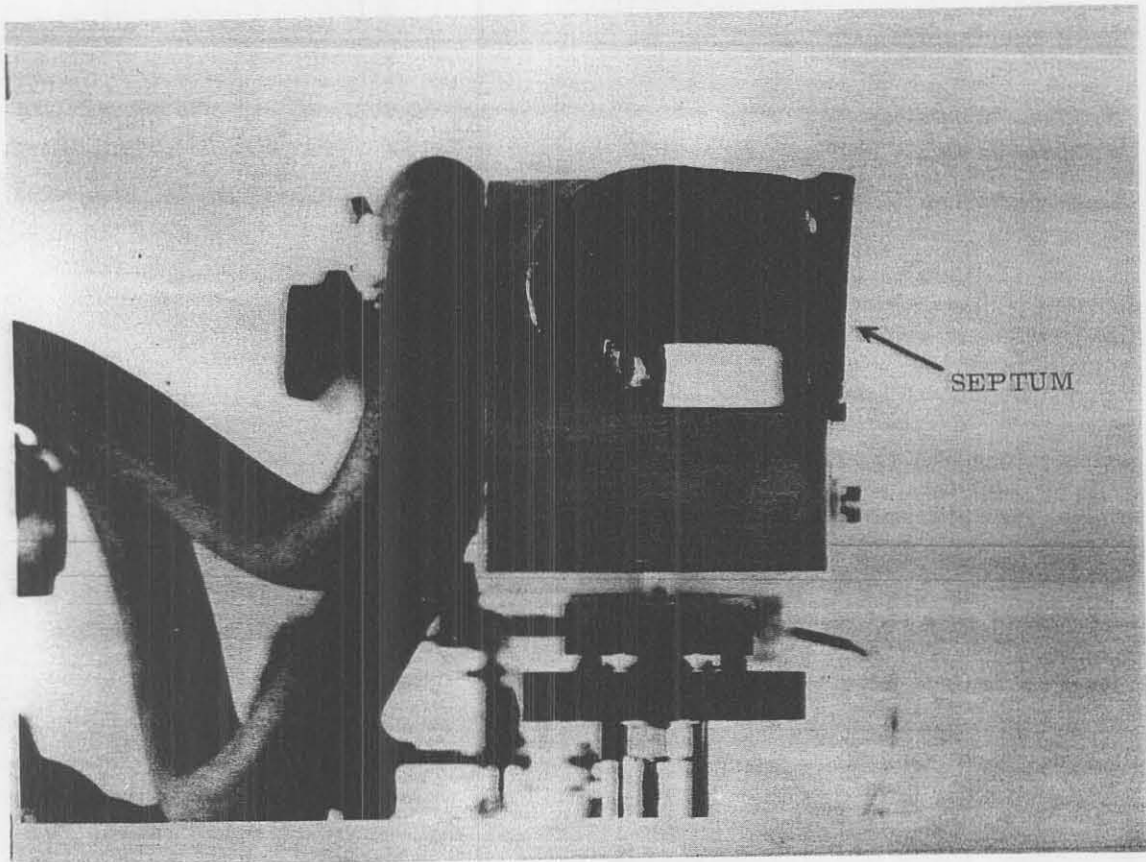


FIG. 9 - "Hard" magnet (front view).



The device (see fig. 4) consists of two targets, with radial width 1 mm and 5 mm, placed at different radial and azimuthal positions. With this detecting system, when the electrons spiralize inward in absence of the field index perturbation, the  $\gamma$  ray beam comes out only from the first target (1 mm width), nearer to the central orbit. If at the same time the magnetic perturbation is applied, a  $\gamma$  ray beam (see fig. 5) comes out from the second target too, due obviously to the electrons that jump the first one. The two  $\gamma$ -ray intensities may give a rough estimation of the extraction efficiency.

In our case, the current required to excite the resonance at 1 GeV is about 30 Amperes in each wire, corresponding to a value  $\Delta B_z(x=0) \cong 30$  Gauss. Fig. 6 shows the current pulse and the spill-out shape observed by a scintillation counter.

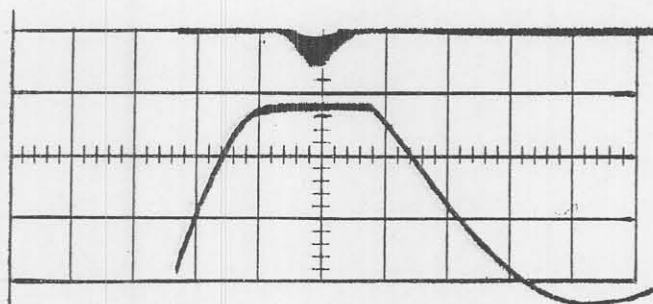
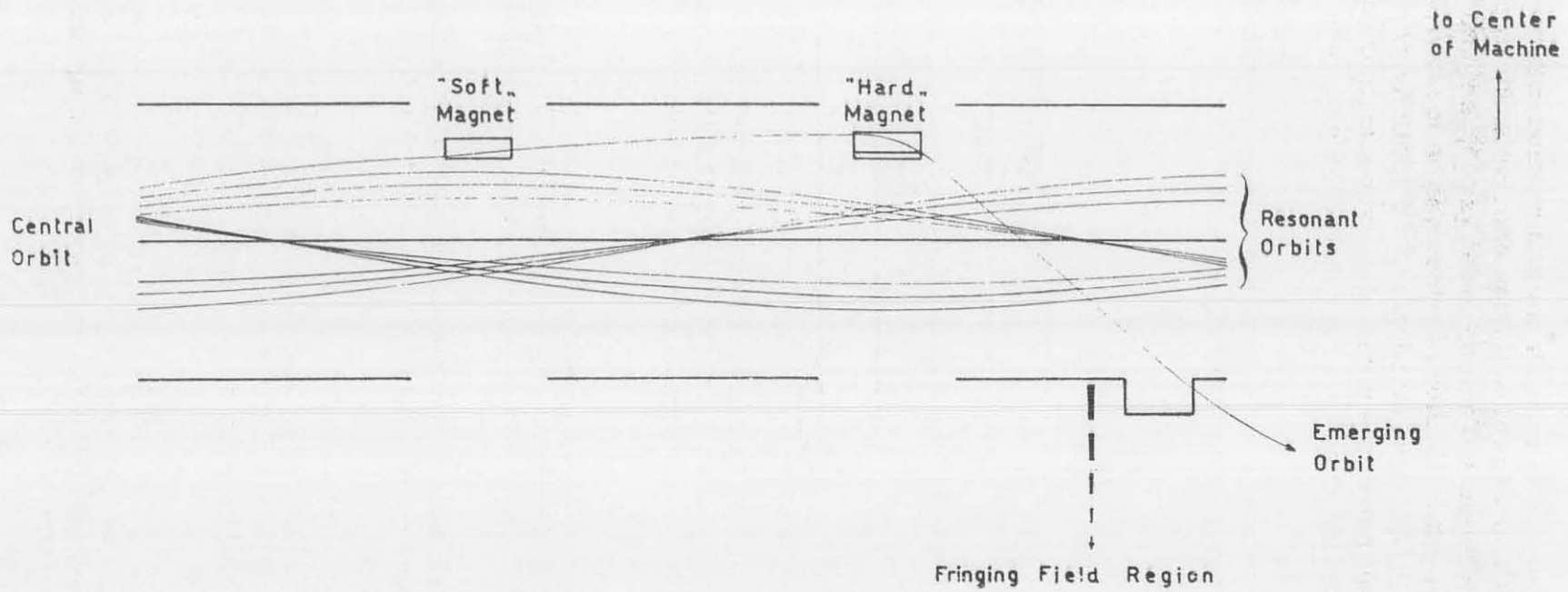


FIG. 6 - Top trace: spill-out shape observed by a scintillator placed near the synchrotron. Bottom trace: current pulse into the correcting coils. Sweep speed: 1 msec/cm.

The extraction system consists of two pulsed septum magnets. The first one ("soft" magnet) is placed in a straight-section of the synchrotron, and deflects the particles slightly towards the center of the machine. The second magnet ("hard" magnet) is placed in the next straight-section, and deflects the electrons outwards, forcing the beam to emerge at the end of the following quadrant (see fig. 7).

The "soft" magnet and its control system are shown in fig. 8. The main characteristics of this magnet are: length 30 cm, gap height 11 mm, gap width 20 mm, septum thickness .5 mm. The field and the current required for 1 GeV extraction are about 550 Gauss and 550 Amperes. The fringing field of the "soft" magnet is less than 10% of the internal field, at 1 mm outside from the septum.

The "hard" magnet is shown in fig. 9. It is similar to the "soft" one, except for the septum thickness, which is 3.5 mm to allow for the water cooling. The field and the current required are 3500 Gauss and 3500 Amperes. The fringing field is less than 3% at 1 mm outside from the septum. In fig. 10 the shape of current pulses in the two magnets is shown. Fig. 11 shows the scheme of the pulser.



Arbitrary Scale

FIG. 7 - Sketch of the extraction system.

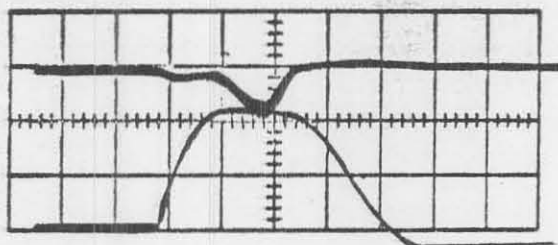


FIG. 10 - Top trace: spill-out shape from a scintillator placed near the electron stopper of the external beam. Bottom trace: shape of the currents injected into both magnets. Sweep speed: 1 msec/cm.

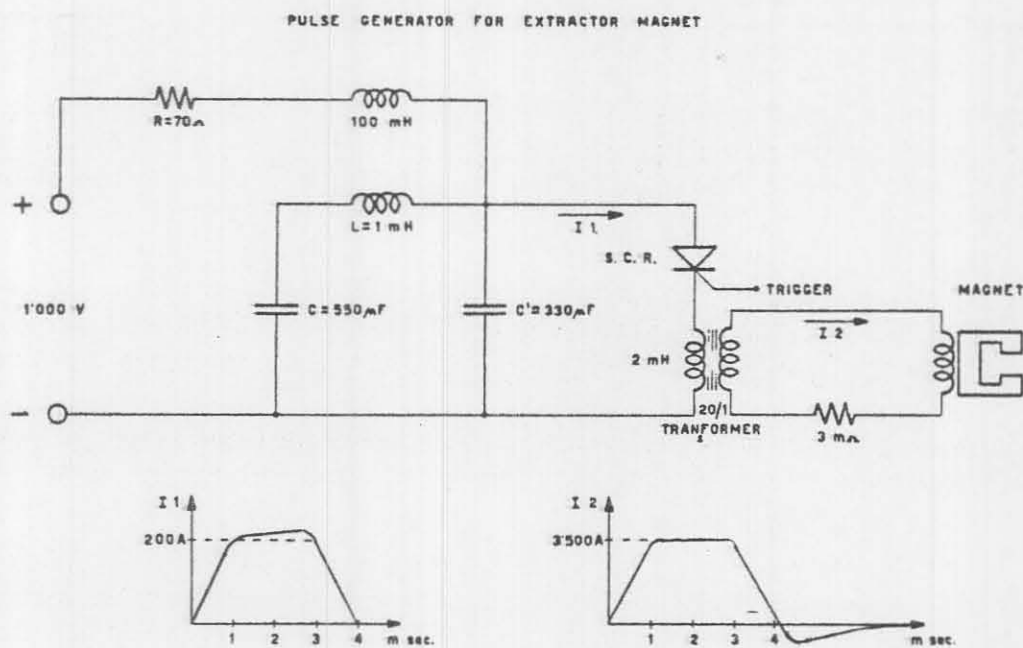


FIG. 11 - Current pulser.

In order to calculate the electron orbits inside the synchrotron's fringing field, the radial dependence of the vertical magnetic field has been measured (the linear shape of the field ends at  $x \approx 7$  cm). A simple analytical expression of  $B_z(x)$ , fitting the measured values of the field in the fringing region, has been introduced into the radial motion equation:

$$(2.2) \quad \frac{d^2x}{d\theta^2} + b(x)x = R(1 - b(x)), \quad \text{where} \quad b(x) = \frac{B_z(x)}{B_0};$$

this one has been numerically integrated by the Runge-Kutta method.

Two orbits calculated in this way are represented in fig. 12. They have zero initial slope and their initial abscissas are -4.5 cm and -5.5 cm. The fringing field has a radial defocusing effect onto the beam. In fact, if the initial radial displacement between two orbits is for instance 1 cm, at the azimuth  $\theta = 90^\circ$  it becomes 6.5 cm.

In order to compensate the fringing field defocusing effect, we have introduced a 3% per cm gradient into the field of the extracting "hard" magnet. In this way a factor 3 reduction of the horizontal beam size has been achieved. Moreover these results gave useful informations for the design of the vacuum chamber and of the beam transport system.

### 3. - CHARACTERISTICS OF THE EXTERNAL BEAM. -

The external beam intensity has been measured by a Wilson quantummeter, and corresponds to about  $10^9$  electrons per pulse, that means that the extraction efficiency is about 50%.

In order to measure the extracted beam emittance, the "minimum spot size" method has been used. The results are about

vertical	emittance = $0.5 \times 10^{-3}$ cm·rad
horizontal	emittance = $2 \times 10^{-3}$ cm·rad.

The main contributions to these values are first, the crossing of 1.5 m length air and second, the variation of the magnet's currents during the long spill-out time.

The momentum spread  $\Delta p/p$  of the external beam has been evaluated by means of a comparison method: the radial width of an undeflected beam has been compared with the radial width of a beam deflected by a zero gradient magnet.

The result for 600 MeV and 100  $\mu$ sec extraction is:

$$\Delta p/p = (1.5 \div 2.0) \times 10^{-3}.$$

Therefore the external beam has practically the same momentum spread of the circulating beam, due to the phase spread of the synchrotron oscillations.

The maximum spill-out time obtained is about 4 msec which corresponds to a duty cycle of  $8 \times 10^{-2}$ .



Scala 1:15

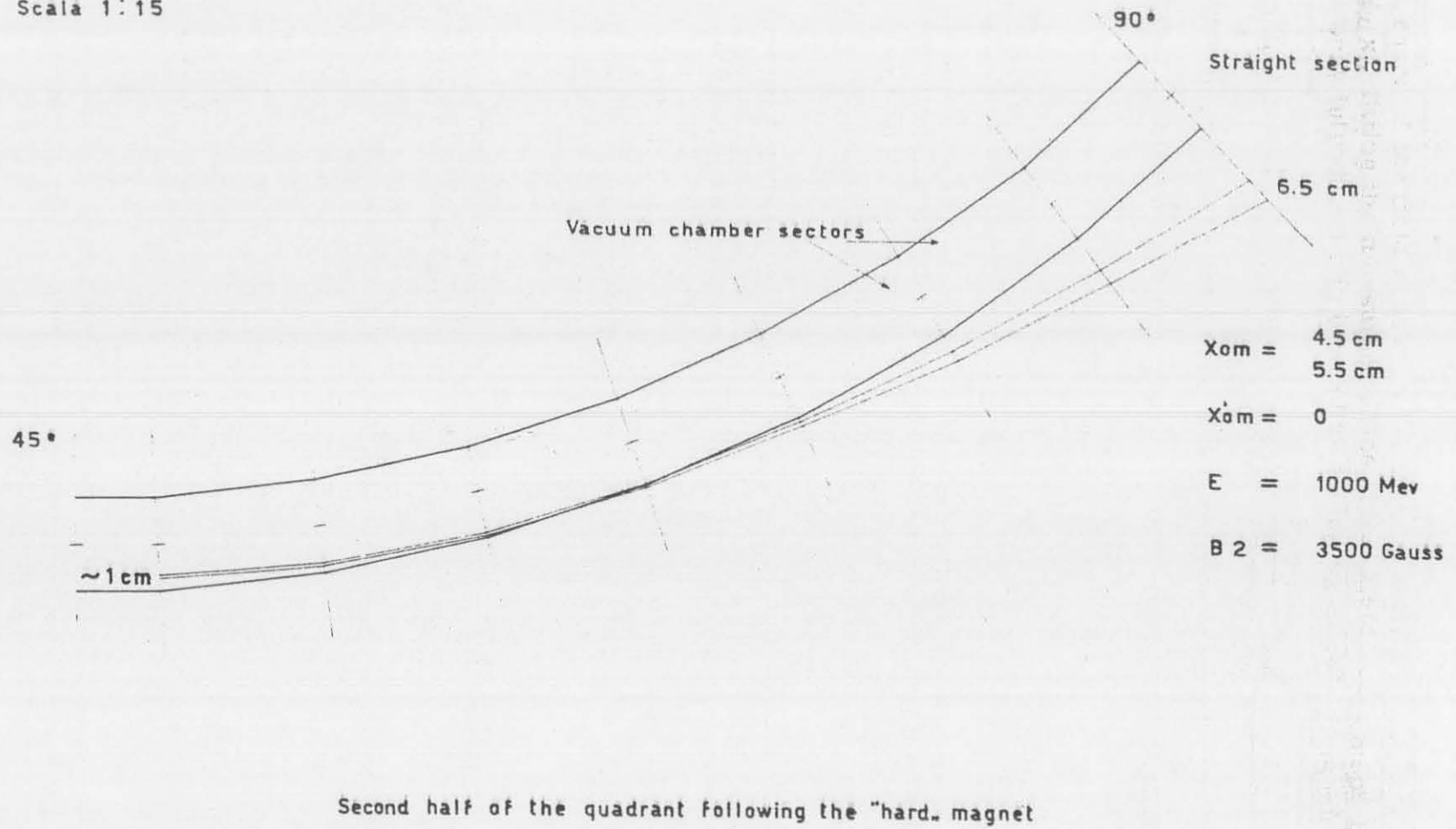


FIG. 12 - Fringing field effect on two orbits with zero initial slope and initial radial displacement = 1 cm.

The authors are particularly grateful and indebted to Mr. L. Cesarini, Mr. M. Spina, and Mr. V. Venturini for their indispensable technical assistance.

## REFERENCES. -

- (1) - H. G. Hereward, Proc. of the Int. Conf. on High Energy Accelerators, Dubna, 1963 (Atomizdat, Moscow, 1964), p. 690.
- (2) - F. W. Brasse, G. E. Fisher, M. Fotino and K. W. Robinson, Proc. of the Int. Conf. on High Energy Accelerators, Dubna, 1963 (Atomizdat, Moscow, 1964), p. 718.
- (3) - U. Bizzarri and A. Turrin, Nuovo Cimento 37, 751 (1965).
- (4) - J. W. Benoit, K. B. Conner, J. Kirchgessner and F. C. Shoemaker, Proc. of the First National Particle Accelerator Conf., Washington, 1965; IEEE Trans. on Nuclear Science NS-12, 926 (1965).
- (5) - J. Kirchgessner, J. W. Benoit and F. C. Shoemaker, presented at the V Int. Conf. on High Energy Accelerators, Frascati, september, 1965.
- (6) - M. Q. Barton, presented at the V Int. Conf. on High Energy Accelerators, Frascati, september, 1965.
- (7) - A. Turrin, Nuovo Cimento 8, 511 (1958).